24. J. S. Kaptein *et al.*, *J. Biol. Chem.* **271**, 18875 (1996).
25. M. Davis, personal communication.
26. EMSA was done as described [C. Peterson, K. Orth, K. Calame, *Mol. Cell. Biol.* **6**, 4168 (1986)]. A 25-bp oligonucleotide corresponding to the c-*myc* PRF site (CGCGTACAGAAAGGGAAAGGACTAG) was used as a probe. Binding mixtures including 3 μg of nuclear extract protein, 1 ng of probe (~100,000 cpm), and 3 μg of poly(dI-dC) were incubated on ice for 30 min, then subjected to electrophoresis in a 6% polyacrylamide gel; for competition or supershift, competitors (50×) or antiserum (1 μl) were incubated with nuclear extracts on ice for 15 min before addition of probe. GATA tetramer [A. Henderson, S. McDougall, J. Leiden, K. Calame, *Mol. Cell. Biol.* **14**, 4286 (1994)] was used as a nonspecific competitor. Antiserum to Blimp-1 was raised against the NH_2-terminus of Blimp-1 and did not cross-react with other zinc finger proteins in protein immunoblot (*15*).
27. M. Bradford, *Anal. Biochem.* **72**, 248 (1976).
28. G. Peterson and J. Mercer, *Eur. J. Biochem.* **160**, 579 (1986).
29. T. Graeber *et al.*, *Nature* **379**, 88 (1996).
30. We thank M. Davis and D. Mack for the Blimp-1 expression plasmid and antiserum to Blimp-1; R. Pine for ISRE and PRD1 oligonucleotides; M. Dorsch for IL-2– and IL-5–containing supernatants; members of our laboratory for helpful discussions; and D. Cobrinik, R. Dalla-Favera, and A. Henderson for critically reading the manuscript. Supported by American Cancer Society (ACS) grant VM108, ACS grant 130, and U.S. Army Medical Research grant 17-94-J-4102 to K.C.

3 December 1996; accepted 27 February 1997

Maintenance of Acetylcholine Receptor Number by Neuregulins at the Neuromuscular Junction in Vivo

Alfred W. Sandrock Jr.,* Stuart E. Dryer,*† Kenneth M. Rosen, Shai N. Gozani, Rainer Kramer, Lars E. Theill, Gerald D. Fischbach‡

ARIA (for acetylcholine receptor–inducing activity), a protein purified on the basis of its ability to stimulate acetylcholine receptor (AChR) synthesis in cultured myotubes, is a member of the neuregulin family and is present at motor endplates. This suggests an important role for neuregulins in mediating the nerve-dependent accumulation of AChRs in the postsynaptic membrane. Nerve-muscle synapses have now been analyzed in neuregulin-deficient animals. Mice that are heterozygous for the deletion of neuregulin isoforms containing an immunoglobulin-like domain are myasthenic. Postsynaptic AChR density is significantly reduced, as judged by the decrease in the mean amplitude of spontaneous miniature endplate potentials and bungarotoxin binding. On the other hand, the mean amplitude of evoked endplate potentials was not decreased, due to an increase in the number of quanta released per impulse, a compensation that has been observed in other myasthenic states. Thus, the density of AChRs in the postsynaptic membrane depends on immunoglobulin-containing neuregulin isoforms throughout the life of the animal.

The fidelity of neuromuscular transmission depends on the extraordinarily high density of AChRs in the postsynaptic muscle membrane. Developmental studies have pointed to the important trophic influence of the motor nerve in the regulation of endplate AChR density (*1*), an effect strong enough to override the suppression of AChR synthesis by muscle activity. Part of the nerve's local influence on AChR density is to promote the immobilization of AChRs, an effect mediated by the glycoprotein agrin (*2*). Another important local influence of the motor nerve is to increase the synthesis and insertion of AChRs into the postsynaptic membrane (*3*). In fact, endplate nuclei in developing and mature muscle are known to transcribe AChR subunit genes at a high rate as compared with that in nonsynaptic nuclei (*4*, *5*). The effect of synthesis on local receptor density remains evident in mice that lack the principal cytoplasmic AChR anchoring protein rapsyn (*6*).

The most likely candidate for mediation of the motor neuron's influence on endplate AChR synthesis is ARIA (for acetylcholine receptor–inducing activity), a protein purified from brain extracts on the basis of its ability to stimulate the synthesis of AChRs in cultured myotubes (*7*, *8*). ARIA is a member of the neuregulin family of ligands for the 185-kD transmembrane receptor tyrosine kinases ErbB2, ErbB3, and ErbB4 (also called Her2, Her3, and Her4), which are closely related to the epidermal growth factor (EGF) receptor (*9*, *10*). Neuregulins are potent activators of muscle AChR synthesis, with a median effective dose (ED_{50}) of 25 to 50 pM (*11*); neuregulin mRNA can be detected in embryonic motor neurons when motor axons first invade peripheral muscle masses (*12*, *13*) and is also abundant in adult motor neurons (*13*); neuregulin receptors are present in skeletal muscle cells and may be concentrated at the neuromuscular junction (*14–16*); neuregulin protein is concentrated in motor nerve terminals (*15–18*) and accumulates in the extracellular matrix of the synaptic cleft (*12*, *15*, *18*); and in mammalian muscle, neuregulin increases mRNA encoding ε (*17*, *19*), an AChR subunit that replaces the γ subunit during development. Neuregulins may therefore mediate the nerve-dependent maturation of junctional AChRs (*20*) as well as enhance overall AChR gene expression at developing and mature nerve-muscle synapses.

More direct evidence of the role of neuregulins at neuromuscular junctions would require the selective inhibition or elimination of neuregulin activity, or both. When mice are genetically altered so that exons encoding the EGF-like domain (*21*) or the immunoglobulin (Ig)-like domain (*22*) of neuregulin or the neuregulin receptors ErbB2 (*23*) and ErbB4 (*24*) have been deleted, homozygous animals die on or about embryonic day 10 (E10) with defects of the heart, cranial ganglia, and hindbrain. This is well before the formation of neuromuscular synapses begins on about E15 (*25*). Heterozygous animals appear normal and are fertile. This, of course, does not exclude a subtle defect at the neuromuscular junctions.

Although brain-purified ARIA contained Ig-domain amino acid sequences, Ig-containing isoforms may represent a small fraction (about 10 to 20%) of the total that are present in motor neurons (*13*, *26*). Other forms, in which a cysteine-rich region replaces the Ig-like domain (Fig. 1A), predominate. We studied mice deficient in Ig-containing neuregulins because these isoforms may be particularly important at the neuromuscular junction. The Ig-like domain binds heparin (*8*, *27*), an affinity that may be responsible for the observed association of neuregulin with the extracellular matrix of the synaptic cleft (*12*, *15*, *18*). Thus, by accumulating at the endplate, Ig-containing neuregulins may exert a major effect on endplate AChR synthesis. In fact, molecules associated with the synaptic basal lamina have been shown to promote the synthesis of AChRs in denervated adult muscle (*28*), and they appear to have a selective effect on the ε-containing (adult)

A. W. Sandrock Jr., Department of Neurobiology, Harvard Medical School, Boston, MA 02115, and Department of Neurology, Massachusetts General Hospital, Boston, MA 02114, USA.
S. E. Dryer, K. M. Rosen, S. N. Gozani, G. D. Fischbach, Department of Neurobiology, Harvard Medical School, Boston, MA 02115, USA.
R. Kramer and L. E. Theill, Amgen, Thousand Oaks, CA 91320, USA.

*These authors contributed equally to this work.
†Present address: Program in Neuroscience, Florida State University, Tallahassee, FL 32306, USA.
‡To whom correspondence should be addressed.

type of AChR (*5*, *29*).

All neuregulin-deficient mice used in this study were derived from founder animals described in the original publication on the disruption of the Ig-like domain of the neuregulin gene by homologous recombination (*22*). Heterozygous (+/–) mice as well as wild-type (+/+) littermates were genotyped by polymerase chain reaction (PCR) analysis of genomic DNA (*22*). The abundance of Ig-containing neuregulin transcripts in the spinal cord was quantified by S1-nuclease protection assay (*30*). Protected fragments that represent Ig-containing neuregulin mRNA were reduced in each of seven heterozygotic animals as compared to five wild-type animals (Fig. 1B). The mean reduction was 45%. The concentration of glyceraldehyde phosphate dehydrogenase (GAPDH) mRNA, which was measured simultaneously as a control, was identical in the two groups (Fig. 1B). Although RNA from the entire spinal cord was analyzed in this experiment, in situ hybridization studies of spinal cord sections have shown that neuregulin mRNA resides largely in motor neurons (*8*, *10*, *12*, *13*, *31*). Therefore, expression of Ig-containing neuregulins is reduced in the motor neurons of the heterozygote animals. In contrast, total neuregulin expression in the spinal cord, as measured by nuclease protection with a probe from the EGF-like domain, was not significantly reduced (Fig. 1C). The expected small reduction (on the order of 5 to 10%) would not have been detected in this assay.

Neuromuscular transmission, assayed by recording compound muscle action potentials (CMAPs) during repetitive nerve stimulation (*32*), was more sensitive to curare in heterozygous animals than in their wild-type littermates. Incremental doses of d-tubocurarine, an AChR antagonist, were intraperitoneally administered at 10-min intervals while trains of stimuli were delivered at 1-min intervals. In the experiment shown in Fig. 2, CMAPs recorded from the heterozygous mouse began to decrease in amplitude 6 min after the 280 nmol per kilogram of body weight (nmol/kg) pulse of curare, whereas those recorded from the wild-type littermate did not decrease until 6 min after the 1120 nmol/kg dose. A decrement in CMAP amplitude reflects the progressive dropout of individual muscle fibers as the evoked endplate potential drops below the threshold of action potential generation. We observed CMAP decreases at significantly lower curare concentrations in the heterozygote mouse in four of the five littermate pairs studied. In one pair, the difference was minimal (only 4 min earlier in the heterozygote animal) and probably insignificant. In the absence of curare, there was no significant decrease in the CMAP amplitude during 3- to 30-Hz trains of 10 stimuli delivered to mice of either genotype.

In a separate set of experiments, single doses of d-tubocurarine were administered to heterozygote and wild-type mice, and trains of CMAP amplitudes were recorded at 1-min intervals for a period of 30 min. In six of seven heterozygote mice (86%), a single intraperitoneal dose of 300 nmol/kg produced at least a 10% decrement between the second and sixth CMAP, whereas only two of seven wild-type animals (29%) exhibited the same CMAP decrease at that dose. Thus, the safety factor of synaptic transmission at heterozygote endplates was reduced, which is consistent with a deficit in the postsynaptic density of AChRs in these animals.

We tested the postsynaptic sensitivity to ACh by measuring the amplitude of spontaneous miniature endplate potentials (MEPPs) with intracellular microelectrodes in isolated diaphragm-phrenic nerve preparations (*33*). As illustrated in Fig. 3, A and B, the mean MEPP was reduced at heterozygote endplates as compared with wild-type controls. Table 1 summarizes the results from four wild-type and four heterozygous mice. On average, there was an approximately 30% reduction in MEPP size (v_1). This difference could not be attributed to a disparity of resting membrane potential (V_m), nor could it be due to differences in

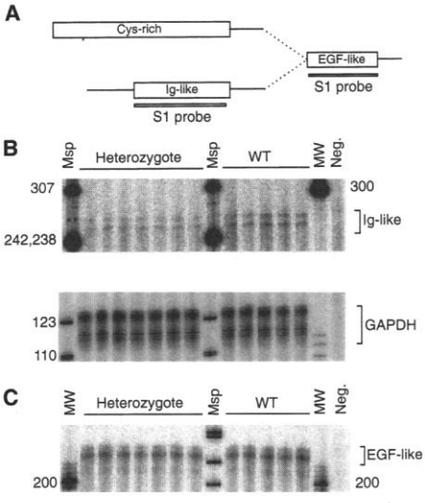

Fig. 1. Heterozygote mice are deficient in Ig-containing neuregulin isoforms. (**A**) The two major splice variants of neuregulin that are NH_2-terminal to the EGF-like domain. One isoform contains an Ig-like domain, and in the other the Ig-like domain is replaced by a region that contains eight cysteine residues. (**B**) Nuclease protection of spinal cord RNA from seven heterozygote and five wild-type (WT) animals with a probe corresponding to the Ig-like domain (*30*). A GAPDH probe was used to measure equivalent loading. Msp, an Msp I digest of pBR322 DNA; MW, a 100–base pair molecular weight ladder (the numbers at left and right indicate length in nucleotides); neg., protection of probes when hybridized to an equivalent weight of yeast RNA. (**C**) Nuclease protection with a probe derived from the EGF-like domain. A simultaneous assay for GAPDH was used to establish equivalence of RNA loading (not shown).

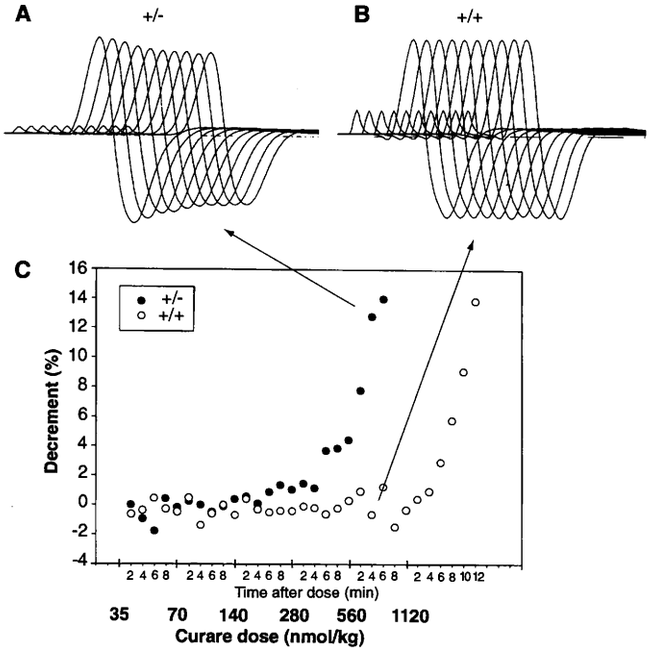

Fig. 2. The safety factor of neuromuscular transmission is reduced in heterozygote mice as compared with that in wild-type mice. CMAPs recorded from forelimb flexor muscles of a heterozygote mouse (**A**) and of a wild-type littermate (**B**) in response to 30-Hz stimulation of the ipsilateral brachial plexus (*8*, *10*, *12*, *13*, *31*). Both records were obtained 4 min after the 560 nmol/kg dose of intraperitoneal curare. (**C**) Complete, timed, incremental dose-response curves. Incremental doses of curare (bold numbers) were administered at 10-min intervals, whereas CMAP responses were recorded at 2-min intervals. The percent decrement is based on the amplitudes of the second and sixth CMAPs during the 30-Hz trains. CMAPs do decrease in wild-type animals, but do so after a delay and an additional, higher dose of curare.

Table 1. Summary of synaptic potentials recorded from wild-type and heterozygous mice.

V_{epp} (mV)	v_1 (mV)	t_{10-90} (ms)	V_m (mV)	m_1	m_2
		Wild-type (n = 4 mice)			
2.33 ± 0.23 (n = 19)	1.05 ± 0.04 (n = 19)	0.97 ± 0.04 (n = 19)	−64 ± 4 (n = 19)	2.23 ± 0.21 (n = 19)	3.48 ± 0.35 (n = 19)
		Heterozygote (n = 4 mice)			
3.06* ± 0.22 (n = 30)	0.76* ± 0.02 (n = 32)	0.95 ± 0.04 (n = 30)	−63 ± 2 (n = 32)	4.03* ± 0.28 (n = 30)	6.48* ± 0.48 (n = 30)

*P < 0.05; different from wild-type value.

placement of the recording electrode relative to the endplate, because the mean rise times of the synaptic potentials (t_{10-90}) were virtually identical (Table 1).

More direct evidence for a reduction in overall endplate AChR density was obtained in α-bungarotoxin binding experiments (*34*). Freshly dissected diaphragms were exposed to saturating concentrations of ^{125}I-bungarotoxin. In one set of experiments, the diaphragms were cut into endplate-rich strips, and the radioactivity was determined in a gamma counter. There were approximately 30% fewer specific counts per minute (total counts per minute minus counts per minute bound in the presence of excess unlabeled α-bungarotoxin) in the endplate-rich hemidiaphragm strips of heterozygote animals as compared with those of wild-type animals [8756 ± 765 cpm, mean ± SEM, n = 6; versus 12,462 ± 949 cpm, n = 6 (P = 0.012)]. In another set of experiments, the diaphragms were teased into fascicles of fewer than five muscle fibers and processed for autoradiography. Clusters of grains were less dense in diaphragms from heterozygote animals than in those from wild-type animals (Fig. 3C). Morphometric analysis of 49 endplates from three wild-type animals and 69 endplates from three heterozygote animals showed some overlap between the two samples. However, the ratio of the mean grain densities was 51%, and this reduction was highly significant (P < 0.001). Each measurement and the means of each group are shown in Fig. 3D. Our results show that AChRs are reduced in number at the neuromuscular junctions of mice that are deficient in Ig-containing neuregulins as compared with those of wild-type mice.

Nerve-evoked endplate potentials (EPPs) were studied under conditions of elevated (12 mM) extracellular Mg^{2+} (*33*), which reduces the probability (p) of ACh release. Surprisingly, the mean evoked EPP response was not reduced at heterozygote endplates (Table 1). Because quantal size is reduced, this implies that more quanta are released per impulse from heterozygote than from wild-type motor nerve terminals. In fact, the mean quantal content calculated from the ratio of mean EPP/mean MEPP was twice as large in heterozygote as compared with wild-type endplates (m_1 in Table 1). The difference in mean quantal content is also reflected in the paucity of failures at heterozygote endplates as compared with wild-type endplates (Fig. 4A). In fact, many heterozygote endplates showed no failures at all during 300 pulses, precluding the calculation of mean quantal content (m) by the method of failures ($m = \ln N/n_0$) based on Poisson statistics. We used another estimate of m that does not rely on the use of failure number. If Poisson statistics apply, then the mean quantal content (m_2) is equal to $1/CV^2$, where CV is the coefficient of variation. Estimates of m_2 showed an approximately twofold increase at heterozygote endplates as compared with wild-type endplates (Table 1). Figure 4B illustrates the disparity between wild-type and heterozygote endplates. The close correlation between the values for m_1 and m_2 suggests that Poisson statistics did apply under our conditions. On the basis of independent estimates of m, we conclude that presynaptic nerve terminals appear to compensate for reduced postsynaptic ACh sensitivity by increasing the number of quanta released per pulse.

The increase in mean quantal content might be due to the compensatory sprouting of motor nerve terminals. However, we found no evidence of an increase in endplate size, as estimated by cholinesterase staining of teased muscle fibers (*35*) (Fig. 4C).

Despite the increase in mean quantal content and the relatively normal EPP amplitudes at heterozygote endplates, the population response (CMAP) declined during repetitive stimulation at lower doses of curare in the heterozygote animals. This is not unexpected, given the direct relation between the rate of decline of transmitter release at neuromuscular junctions and the initial mean quantal content (*36*). When stimulated at a rate of 25 Hz, neuromuscular junctions in the heterozygote mice fatigued more rapidly than in

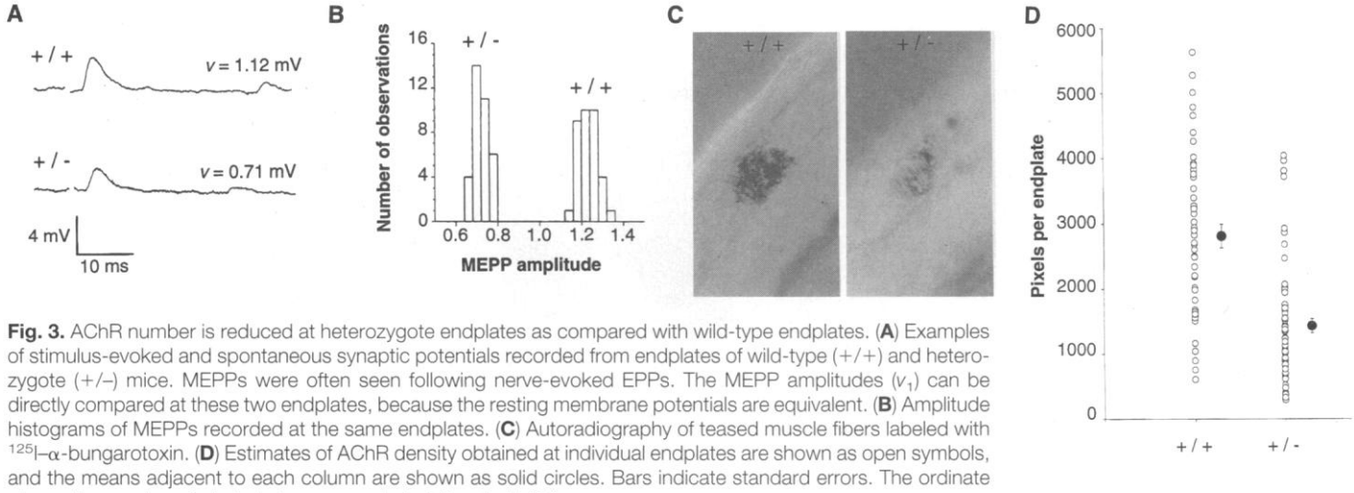

Fig. 3. AChR number is reduced at heterozygote endplates as compared with wild-type endplates. (**A**) Examples of stimulus-evoked and spontaneous synaptic potentials recorded from endplates of wild-type (+/+) and heterozygote (+/–) mice. MEPPs were often seen following nerve-evoked EPPs. The MEPP amplitudes (v_1) can be directly compared at these two endplates, because the resting membrane potentials are equivalent. (**B**) Amplitude histograms of MEPPs recorded at the same endplates. (**C**) Autoradiography of teased muscle fibers labeled with ^{125}I–α-bungarotoxin. (**D**) Estimates of AChR density obtained at individual endplates are shown as open symbols, and the means adjacent to each column are shown as solid circles. Bars indicate standard errors. The ordinate shows the number of pixels below a preselected threshold (*34*).

wild-type mice (37) (Fig. 5). In these experiments, extracellular Mg^{++} was reduced from 12 mM to physiologic levels (1 mM), so that neurotransmitter release was not suppressed. The size of EPPs was reduced with concentrations of d-tubocurarine just sufficient to block action potential generation.

We have shown that neuregulin-deficient mice have a reduced safety factor of neuromuscular transmission. Intracellular microelectrode recordings of MEPP amplitudes, as well as measurements of ^{125}I–α-bungarotoxin binding, indicate that the myasthenia is due to the loss of AChRs from the postsynaptic muscle membrane. Our data provide the most direct evidence to date that neuregulins play a crucial role in maintaining AChR number at motor endplates in vivo.

The heterozygote knockout animals studied here appear to express diminished levels only of neuregulin isoforms with an Ig-like domain. These isoforms represent a small minority of the total, and the remainder (that is, forms that substitute the Ig-like domain with the Cys-rich motif) are presumably biologically active. Our results suggest that Ig-containing isoforms of neuregulin are present in limiting amounts at neuromuscular junctions and are crucial in maintaining postsynaptic AChR density at neuromuscular junctions. This may be the result of the immobilization of this isoform to extracellular matrix components of the synaptic cleft. Thus, although the EGF-like domain appears to be sufficient for activating neuregulin receptors, the free ligand may be less effective in influencing synapse formation in vivo, perhaps because it cannot be concentrated near its site of action.

We observed an increase in the release of ACh at the neuromuscular junctions of heterozygous animals, an apparent compensatory response to the loss of postsynaptic ACh sensitivity, which is mediated by an unknown retrograde signal. A similar phenomenon has been observed in an experimental model of myasthenia gravis (38) and in biopsies of human muscle from patients with myasthenia gravis (39). The augmented transmitter release, although adequately compensating for the loss of AChRs during low rates of motor nerve stimulation, increases the likelihood of synaptic failure during prolonged, high rates of stimulation. The compensation was not caused by an enlargement of the endplate. Thus, the increased quantal content of nerve-evoked ACh release in the heterozygote animals probably reflects an increase in the amount of ACh released per unit length of nerve terminal. It remains to be determined whether this is the result of an increase in the number of release sites or of an increase in the probability of release at each site.

Our results imply that the continued activation of AChR genes in subsynaptic nuclei by neuregulin is critical for the maintenance of postsynaptic AChR density at adult endplates, despite the decrease in AChR turnover during development and despite the ability of agrin to immobilize AChRs in the synapse. In fact, neuregulin-like immunoreactivity remains high at adult neuromuscular junctions (*15*, *18*). The fact that the decrease in neuregulin gene expression is roughly proportional to the loss of AChR number at endplates implies that postsynaptic ACh responses are closely linked to the rate of AChR synthesis and insertion into the postsynaptic membrane (*2*). We do not yet know when the deficit in neuromuscular transmission first becomes evident in the neuregulin-deficient mice during development. Indeed, neuregulin genes are expressed in motor neurons early enough to affect initial neuromuscular synapse formation (*8*, *12*, *13*). Studies of neuregulin-deficient mice during development will shed light on when neuregulin action first becomes essential at neuromuscular junctions.

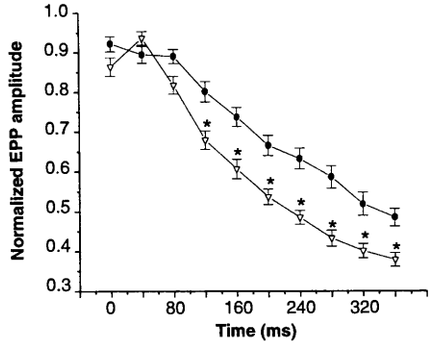

Fig. 5. Evoked EPPs decay more rapidly at heterozygote endplates (open triangles) than at wild-type endplates (solid circles). These experiments were recorded in normal Mg^{2+} (1 mM) with synaptic transmission blocked by curare. EPP amplitudes were normalized to the highest amplitude obtained during the tetanus, which was delivered at 25 Hz. Each point on the wild-type curve represents the mean of 29 endplates in nine mice, and each point on the heterozygote curve represents the mean of 35 endplates in nine mice. Asterisks mark significant differences ($P < 0.05$).

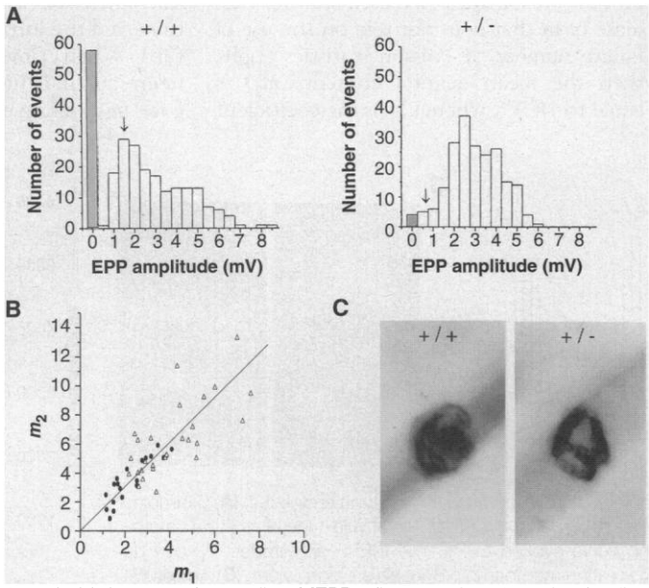

Fig. 4. The number of quanta released per impulse is increased at heterozygote endplates as compared with wild-type controls. (**A**) Amplitude histograms of nerve-evoked EPPs recorded in high extracellular Mg^{2+}. The shaded bar indicates the number of failures (no response after nerve stimulation). (**B**) Mean quantum content calculated as $1/(CV)^2$ (m_2) as a function of mean quantum content calculated as mean V_{epp}/mean v_1 (m_1). The quantal content calculated by either method is higher at heterozygote endplates (open triangles) than at wild-type endplates (solid ovals). The slope of this relation is slightly greater than 1, probably because the smallest MEPPs disappear into the noise, leading to an underestimate of m_1; and because the smallest evoked responses are also lost, leading to an overestimate of m_2. (**C**) Overall endplate size, revealed by cholinesterase histochemistry, does not differ between wild-type and heterozygote animals.

REFERENCES AND NOTES

1. Z. W. Hall and J. R. Sanes, *Cell* **72**/*Neuron* **10** (suppl.), 99 (1993).
2. U. J. McMahan, *Cold Spring Harbor Symp. Quant. Biol.* **55**, 407 (1990); M. Gautam *et al.*, *Cell* **85**, 525 (1996).
3. L. W. Role, V. R. Matossian, R. J. O'Brien, G. D. Fischbach, *J. Neurosci.* **5**, 2197 (1985).
4. J. P. Merlie and J. R. Sanes, *Nature* **317**, 66 (1985); D. Goldman and J. Staple, *Neuron* **3**, 219 (1989); J. R. Sanes *et al.*, *Development* **113**, 1181 (1991); A. M. Simon, P. Hoppe, S. J. Burden, *ibid.* **114**, 545 (1992).
5. H. R. Brenner, A. Herczeg, C. R. Slater, *Development* **116**, 41 (1992).
6. M. Gautam *et al.*, *Nature* **377**, 232 (1995).
7. T. M. Jessell, R. E. Siegel, G. D. Fischbach, *Proc. Natl. Acad. Sci. U.S.A.* **76**, 5397 (1979); M. H. Buc-Caron, P. Nystrom, G. D. Fischbach, *Dev. Biol.* **95**, 378 (1983); T. B. Usdin and G. D. Fischbach, *J. Cell Biol.* **103**, 493 (1986); G. D. Fischbach and K. M. Rosen, *Annu. Rev. Neurosci.*, in press.
8. P. L. Falls *et al.*, *Cell* **72**, 801 (1993).

9. W. E. Holmes *et al.*, *Science* **256**, 1205 (1992); D. Wen *et al.*, *Cell* **69**, 559 (1992).
10. M. A. Marchionni *et al.*, *Nature* **362**, 312 (1993).
11. K. M. Rosen *et al.*, *Cold Spring Harbor Symp. Quant. Biol.*, in press.
12. A. D. J. Goodearl *et al.*, *J. Cell Biol.* **130**, 1423 (1995).
13. G. Corfas *et al.*, *Neuron* **14**, 103 (1995).
14. N. Altiok, J. L. Bessereau, J. P. Changeux, *EMBO J.* **14**, 4258 (1995); X. J. Zhu, C. Lai, S. Thomas, S. J. Burden, *ibid.*, p. 5842.
15. S. A. Jo, X. Zhu, M. A. Marchionni, S. J. Burden, *Nature* **373**, 158 (1995).
16. L. M. Moscoso *et al.*, *Dev. Biol.* **172**, 158 (1995).
17. G. C. Chu, L. M. Moscoso, M. X. Sliwkowski, J. P. Merlie, *Neuron* **14**, 329 (1995).
18. A. W. Sandrock *et al.*, *J. Neurosci.* **15**, 6124 (1995).
19. J. C. Martinou, D. L. Falls, G. D. Fischbach, J. P. Merlie, *Proc. Natl. Acad. Sci. U.S.A.* **88**, 7669 (1991).
20. H. R. Brenner and B. Sakmann, *Nature* **271**, 366 (1978); *J. Physiol. (London)* **337**, 159 (1983); H. R. Brenner, V. Witzemann, B. Sakmann, *Nature* **344**, 544 (1990).
21. D. Meyer and C. Birchmeier, *ibid.* **378**, 386 (1995).
22. R. Kramer *et al.*, *Proc. Natl. Acad. Sci. U.S.A.* **93**, 4833 (1996).
23. K. Lee *et al.*, *Nature* **378**, 394 (1995).
24. M. Gassman *et al.*, *Nature* **378**, 390 (1995).
25. M. J. Dennis, L. Ziskind-Conhaim, A. J. Harris, *Dev. Biol.* **81**, 266 (1981).
26. Y. Kuo, X. Yang, L. Role, *Soc. Neurosci. Abstr.* **20**, 452.18 (1994); W.-H. Ho *et al.*, *J. Biol. Chem.* **270**, 14523 (1995).
27. J. A. Loeb and G. D. Fischbach, *J. Cell Biol.* **130**, 127 (1995).
28. S. J. Burden, P. B. Sargent, U. J. McMahan, *ibid.* **82**, 412 (1979).
29. D. Goldman, B. M. Carlson, J. Staple, *Neuron* **7**, 649 (1991).
30. A cDNA clone encoding the majority of the extracellular domain of a mouse neuregulin β was generated by reverse transcription–polymerase chain reaction (RT-PCR) of mouse spinal cord RNA with the following primers: sense 5′-CAGATTGAAAGAAATGAAGAGCC-3′ and antisense 5′-CACCACACACATGATGCCGAC-3′. PCR was performed as described [K. H. Hecker and K. H. Roux, *Biotechniques* **20**, 478 (1996)]. The PCR product was cloned with the use of the TA cloning system (Invitrogen, San Diego, CA). The cDNA fragment was then cloned into bacteriophage M13mp19, and a sense strand containing viral DNA was used for the synthesis of an antisense DNA probe. Ig-like and EGF-like domain probes were synthesized in the presence of 20 μCi each of ^{32}P–α-dCTP and -dATP (800 Ci/mmol; NEN, Boston, MA). The Ig probe reaction was primed with an antisense primer derived from near the end of the Ig-like domain sequence of the cDNA (5′-GACTCAACAATGGTGATG-3′). The EGF-like probe reaction was primed with the M13 universal primer. A control antisense GAPDH probe of 125 nucleotides was synthesized in essentially the same manner, except that only ^{32}P–α-dATP was included. Five micrograms of total RNA from seven heterozygous and five wild-type animals were evaporated to dryness in the presence of 150,000 disintegrations per minute (dpm) of a gel-purified, domain-specific, neuregulin probe and 50,000 dpm of GAPDH probe. The samples were dissolved in 10 μl of hybridization buffer (75% formamide, 0.5 M NaCl, 40 mM PIPES (pH 6.4), 1 mM EDTA, and 0.05% SDS), heated to 95°C for 2 min, and hybridized for more than 18 hours at 52°C. For digestion, the samples were diluted into 400 μl of digestion buffer [200 mM NaCl, 30 mM sodium acetate (pH 4.5), and 5 mM $ZnSO_4$] containing S1 nuclease (350 U/ml) (Pharmacia, Piscataway, NJ), and the reactions were incubated for 1 hour at 37°C. The products were separated by electrophoresis on DNA sequencing gels and visualized with a phosphorimager screen (Molecular Dynamics, Sunnyvale, CA) exposed for 24 to 72 hours. The density of equivalent areas was determined, and values for relative neuregulin levels were expressed as the ratio to the signal for GAPDH.
31. A. Orr-Urteger *et al.*, *Proc. Natl. Acad. Sci. U.S.A.* **90**, 1867 (1993); M. S. Chen *et al.*, *J. Comp. Neurol.* **349**, 389 (1994); D. Meyer and C. Birchmeier, *Proc. Natl. Acad. Sci. U.S.A.* **91**, 1064 (1994).
32. General anesthesia was induced in mice with isoflurane and maintained with a 1% (v/v) isoflurane-oxygen mixture flowing at a rate of 200 cm^3/min. Two 26G monopolar needle electrodes (Nicolet, Madison, WI) were inserted into the anterior axillary region in order to supramaximally stimulate the brachial plexus with 5- to 10-mA constant current pulses of 200 μs duration (WPI A360, Sarasota, FL). Trains of 10 stimuli were delivered at frequencies of 3 or 30 Hz. CMAPs were recorded with a 24G monopolar needle electrode (Nicolet) inserted into the flexor muscle compartment of the ipsilateral forelimb and were amplified with a low noise differential amplifier (WPI Isodam, Sarasota, FL). A small disposable surface electrode (Nicolet) attached to the skin of the forepaw served as the reference electrode for the differential measurement. Another disposable surface electrode was attached to the tail to serve as the ground. For systemic curare infusions, a 27G butterfly catheter was inserted into the peritoneal cavity through a small skin incision. Incremental doses (35, 70, 140, 280, 560, and 1120 nmol/kg) of d-tubocurarine chloride (Sigma) in 0.5 to 1.0 ml of 0.9% NaCl were injected through the catheter every 10 min (the catheter was flushed with 1 ml saline after each injection). During the timed curare infusions, trains of 10 repetitive nerve stimulations (3 Hz alternating with 30 Hz) were performed at 1-min intervals, and the ratio of amplitudes of the second to sixth CMAPs was calculated online.
33. Mouse hemidiaphragms were pinned out in a chamber perfused with a balanced salt solution containing 150 mM NaCl, 5.4 mM KCl, 12 mM $MgCl_2$, 2 mM $CaCl_2$, 10 mM Hepes-NaOH, and 13 mM glucose (pH 7.4) at room temperature (22° to 24°C). The elevated Mg^{2+} was sufficient to reduce the evoked EPP to below the action potential threshold. Phrenic nerves were drawn into a fine capillary-stimulating electrode. Intracellular recordings were made with microelectrodes that measured 20 to 70 megohm when filled with 3 M KCl. The muscle was penetrated under direct visual control near the main intramuscular nerve or a fine side branch; the electrode was then repositioned to maximize the amplitude and rate of rise of the evoked EPP. At the optimal position, a series of 50 to 300 EPPs evoked at a rate of 1 Hz were collected. Spontaneously occurring MEPPs (10 to 35 per endplate) were recorded before, during, and after the periods of nerve stimulation. All data were digitized at 25 kHz and stored on magnetic disks with the use of Axotape software (Axon Instruments). The amplitudes of spontaneous and evoked synaptic potentials were determined with the use of PCLAMP software (Axon Instruments). Quantal parameters were estimated by two independent methods. One estimate (m_1) was obtained by dividing the mean amplitude of the evoked EPPs by that of the MEPPs. A second estimate (m_2) was calculated as $1/(CV)^2$, where CV is the coefficient of variation of 50 to 300 evoked EPPs. The calculation of m_2 is accurate under conditions in which the Poisson probability law describes the statistics of transmitter release. The concentration of Mg^{2-} in the bath solution was selected with this in mind. Because most endplate responses were less than 5 mV, no corrections were made for nonlinear summation of synaptic potentials.
34. Mice were killed by an overdose of isoflurane, and diaphragms were dissected, rinsed with phosphate-buffered saline (PBS), and incubated for 2 hours at room temperature with 2 nM ^{125}I–α-bungarotoxin (Amersham; specific activity = 2000 Ci/mmol) in Puck's saline solution containing 1 mg of bovine serum albumin (BSA) per milliliter. The diaphragms were then rinsed four times (15 min each) with PBS and fixed for 15 min at room temperature with 3% glutaraldehyde in 0.1 M phosphate buffer (pH 7.4). After being rinsed in L15 medium (Gibco) containing BSA (1 mg/ml), the diaphragms were divided midsagittally into hemidiaphragms. In some experiments, endplate-rich strips (measuring approximately 20 × 1.5 mm) were prepared from each hemidiaphragm by cutting along either side of the main intramuscular branch of the phrenic nerve. These strips were immersed in 0.5 ml of PBS, and the radioactivity was determined in a gamma counter. Specific α-bungarotoxin binding was calculated by subtracting counts per minute found in endplate-rich strips of diaphragms that had been incubated with excess unlabeled α-bungarotoxin. In other experiments, hemidiaphragms were immersed in 30% sucrose in PBS overnight at 4°C before being placed on microscope slides (SuperFrost Plus, Fisher Scientific) where they were teased into fascicles of fewer than five muscle fibers with a pair of fine forceps. After drying, the teased fibers were rinsed with distilled water and the slides were dipped in a 1:1 mixture of NT-3B emulsion (Kodak) with water. The slides were placed in a desiccated, light-tight slide box and stored at 4°C for 8 hours before being developed, fixed, dehydrated with ethanol and xylene, and cover-slipped in Cytoseal (VWR Scientific Products, Bridgeport, NJ). For the photomicrographs of Fig. 3C, endplates were photographed on 35-mm color slide film under Nomarski optics. For morphometric studies, bright-field images were captured with a charge-coupled device (CCD) camera (Hamamatsu). With a 20× objective lens, most of the grains at each endplate were in sharp focus. Monochromatic (gray-scale) digitized images only of endplates viewed *en face* were collected with Image-1 software (Corel). With the use of SigmaScanPro software (Jandel Scientific), a box was drawn around the endplate, and a 0 to 100% intensity scale was created for each image. The number of pixels that fell below a 50% intensity level were counted. This intensity threshold was chosen because it gave accurate grain counts. Statistical significance was estimated with the Mann-Whitney rank sums test with the use of SigmaStat (Jandel Scientific).
35. Mice were killed by an overdose of isoflurane, and diaphragms were dissected, rinsed with PBS, fixed for 15 min with 3% glutaraldehyde in 0.1 M phosphate buffer (pH 7.4), immersed in 30% sucrose in PBS overnight at 4°C, and teased into fascicles of fewer than five muscle fibers, as described above. After drying, the slides were dipped into a reaction mixture containing acetylthiocholine iodide (0.5 mg/ml), 100 mM sodium citrate, and 30 mM cupric sulfate in 0.1 M sodium maleate buffer (pH 6.0). The reaction was activated by the addition of 10% (v/v) 5 mM potassium ferricyanide. After reacting for 20 to 30 min at room temperature, the slides were rinsed with PBS, dehydrated with ethanol and xylene, and cover-slipped in Cytoseal (VWR). In control experiments, acetylthiocholine iodide was replaced with butyrylthiocholine iodide. For the photomicrographs of Fig. 4C, AChE-stained endplates were photographed on 35-mm color slide film under bright-field optics. For morphometric studies, bright-field images were captured with a CCD camera (Hamamatsu) equipped with an intensifier. Monochromatic (gray-scale) digitized images only of endplates viewed *en face* were collected using Image-1 software (Corel). Using SigmaScanPro software (Jandel Scientific), a 0 to 100% intensity scale was created and the area occupied by pixels falling below a 35% intensity level was calculated. This intensity threshold accurately defined the boundaries of AChE-stained endplates. Statistical comparisons were made using SigmaStat (Jandel Scientific).
36. A. Mallart and A. R. Martin, *J. Physiol. (London)* **196**, 593 (1968).
37. Changes in synaptic strength during repetitive stimulation were analyzed in a balanced salt solution similar to that described above, except that it contained 1 mM $MgCl_2$ and 2 mM $CaCl_2$, so that transmitter release was not reduced. In these experiments, neuromuscular transmission was blocked postsynaptically with d-tubocurarine (1.0 to 1.5 μg/ml) (Sigma) in order to keep evoked EPPs below the action potential threshold. Trains of stimuli were delivered at 25 Hz.
38. J. J. Plomp; G. T. van Kempen, P. C. Molenaar, *J. Physiol. (London)* **458**, 487 (1992); *ibid.* **478**, 125 (1994).
39. S. G. Cull-Candy, R. Miledi, A. Trautmann, O. D. Uchitel, *ibid.* **299**, 621 (1980); J. J. Plomp *et al.*, *Ann. Neurol.* **37**, 627 (1995).

40. Supported by grants from NIH National Institute of Neurological Disorders and Stroke awarded to G.D.F. (R01-NS18458) and to A.W.S. (K08-NS01580). We thank D. Kane of Amgen for genotyping and shipping the mice.

20 December 1996; accepted 5 March 1997